J Inorg Organomet Polym (2013) 23:89–94
DOI 10.1007/s10904-012-9744-2

Magnetic Properties of Cobalt-Containing Diblock Copolymers with Cylindrical Morphology of Different Domain Sizes

Yongping Zha · Raghavendra R. Maddikeri · Samuel P. Gido · Gregory N. Tew

Received: 17 July 2012 / Accepted: 21 August 2012 / Published online: 12 September 2012

Abstract Previously, we have synthesized a cobalt-containing diblock copolymer system which exhibited room temperature ferromagnetic properties after phase separation and heat treatment. We have also shown that the morphology and cobalt density in the nanostructured domains both influenced the magnetic properties of these materials due to nanoconfinement which enhanced the dipolar interactions between otherwise superparamagnetic cobalt nanoparticles. Here, we investigated the effect of domain size on the magnetic properties of these room temperature ferromagnetic materials (RTFMs) using a series of five cobalt-containing diblock copolymers with various molecular weights and constant block ratios. The diblock copolymers self-assembled into cylindrical morphologies with different domain sizes upon solvent annealing, and then were converted to RTFMs upon a simple heat treatment. The domain sizes of these RTFMs did not show a significant impact on their coercivity values, possibly because the domain size range investigated was not large enough and the cobalt–cobalt dipolar interactions were nearly constant throughout. At the same time, this study confirms that the RTFMs generated from these novel block copolymers are robust.

Keywords Nanostructured magnetic materials · Cobalt-containing diblock copolymers · Self-assembly · Morphology · Domain size

1 Introduction

Nanostructured magnetic materials have attracted intense research interest recently, as they often exhibit novel and enhanced properties over their bulk counterparts [1–4]. They are of both scientific and practical importance in many areas ranging from microelectronics to biomedical applications [5–8]. Conventional "top-down" techniques, such as photolithography, electron-beam lithography, and X-ray lithography, usually involve multiple steps and expensive instrumentations [9]. On the other hand, metal-containing polymers effectively integrate the redox, magnetic, optical or reactive properties of organometallic complexes with the physical properties of carbon-based polymers [10–13]. Incorporating inorganic elements into self-assembled block copolymers (BCPs) is emerging as a cost-effective and rapid "bottom-up" method for fabricating nanostructured magnetic materials [14–16].

Recently, we reported a straightforward method to generate room temperature ferromagnetic materials (RTFMs) from nanostructured BCPs with cobalt nanoparticles confined to one specific phase [17]. The cobalt-containing diblock copolymers were synthesized via ring-opening metathesis polymerization (ROMP), which is a living polymerization technique and tolerant to the dicobalt hexacarbonyl metal complex embedded in the monomer [18]. Further studies illustrated that the room temperature ferromagnetic (RTF) behavior of the nanostructured BCP materials arose from the enhanced dipolar interactions under nanoconfinement between the otherwise superparamagnetic

Electronic supplementary material The online version of this article (doi:10.1007/s10904-012-9744-2) contains supplementary material, which is available to authorized users.

This paper is dedicated to Prof. Dr. Hiroshi Nishihara for his outstanding contribution to the field of metal-containing polymers.

Y. Zha · R. R. Maddikeri · S. P. Gido · G. N. Tew (✉)
Department of Polymer Science and Engineering,
University of Massachusetts, Amherst, MA 01003, USA
e-mail: tew@mail.pse.umass.edu

cobalt nanoparticles. Both the morphology and cobalt density in the domains were shown to influence the magnetic properties of these materials. In these studies, however, the domain sizes were always held constant for each morphology. In order to fully understand the structure dependence of the magnetic properties for these nanostructured BCP materials, the effect of domain size was considered.

In this communication, a series of five BCPs with an alkyl-functionalized (C_{16}) first block and a cobalt-containing (Co) second block were synthesized by ROMP. The molar ratios of the C_{16} units to the Co units were kept constant (70:30) to provide the same phase-separated morphology. The cylindrical morphology was chosen here as it was previously shown to have the highest coercivity [17]. The domain size (diameter of the cylinders) of the cobalt-containing cylinders was changed from 16 to 25 nm by varying the overall molecular weight of the BCPs from 52 to 296 kDa. Magnetization versus field (*M–H*) measurements were performed for the nanostructured BCP materials using a superconducting quantum interference device (SQUID) magnetometer. All five samples exhibited RTF properties, and their coercivity as a function of the cylindrical domain size was investigated.

2 Experimental

2.1 Materials

All reagents were used as received unless otherwise noted. Triphenylphosphine (Ph_3P), 1-hexadecanol, propargyl alcohol, and ethyl vinyl ether were purchased from Alfa Aesar. Diisopropyl azodicarboxylate (DIAD) and dicobalt octacarbonyl were purchased from Acros Organics. Tetrahydrofuran (THF), dichloromethane (DCM), and methanol were all purchased from Fisher Chemical. THF and DCM were distilled over Na^0/benzophenone and CaH_2 prior to use, respectively. Second generation Grubbs' catalyst (G2) was purchased from Sigma-Aldrich. Third generation Grubbs' catalyst (G3) [19], *exo*-oxanorbornene (**1**) [20], and monomers **2**–**4** [17] were synthesized according to the literature.

2.2 Instruments

The ^1H and ^{13}C NMR spectra were recorded on a Bruker DPX-300 MHz spectrometer. Chemical shifts are expressed in δ (ppm) using residual solvent protons or TMS as internal standard. Molecular weights and polydispersity indexes (PDIs) were measured by gel permeation chromatography (GPC) equipped with two-column sets (Polymer Laboratories) and refractive index (RI) detectors (HP1047A) using THF as mobile phase with a flow rate of 1 mL/min, relative to polystyrene standards.

2.3 Preparation of Cobalt-Containing Diblock Copolymers with Various Molecular Weights and Constant Block Ratios (**Poly1–Poly5**)

Representative synthesis of **Poly1**: Monomers **2** (0.27 g, 0.70 mmol) and **4** (0.15 g, 0.30 mmol) were added into two separate Schlenk flasks under an atmosphere of nitrogen, and dissolved in anhydrous DCM (1 mL/100 mg of monomer). A desired amount of G3 (0.006 g, 0.007 mmol) was added into another Schlenk flask, flushed with nitrogen, and dissolved in a minimum amount of anhydrous DCM. All three solutions were degassed three times by freeze–pump–thaw cycles. First, monomer **2** was transferred to the flask containing the catalyst via cannula. The reaction mixture was stirred vigorously for 5 min, after which an aliquot was taken for GPC analysis, and monomer **4** was transferred to the flask via cannula. The polymerization was allowed to continue for another 5 min, and then quenched with 0.2 mL of ethyl vinyl ether. An aliquot was taken for GPC analysis, and the remaining product was precipitated from methanol. The pure polymer was obtained as red fibers. Yield: 90 % ^1H NMR (300 MHz, $CDCl_3$): δ 6.20–5.95 (br, 1H), 5.93–5.60 (br, 1.14H), 5.20–4.91 (br, 1.15H), 4.90–4.68 (br, 0.65H), 4.63–4.30 (br, 0.74H), 3.65–3.10 (m, 3.10H), 1.85–0.50 (m, 20.92H). ^{13}C NMR (75 MHz, $CDCl_3$): δ 199.9, 176.0, 132.5, 117.7, 53.5, 32.0, 29.7, 27.7, 26.8, 22.7, 14.1. THF GPC: $M_n = 52$ kDa, $M_w/M_n = 1.11$. The other four diblock copolymers, **Poly2–Poly5**, were synthesized by the same method except that the catalyst loading was reduced and the polymerization time was prolonged accordingly with increasing molecular weight.

2.4 Solvent Annealing

Bulk samples (ca. 1 cm × 1 cm × 1 mm) were cast in a Teflon mold from 10 wt% polymer solutions in chloroform, a nonselective solvent for both the C_{16} and Co blocks. The samples were allowed to dry slowly at room temperature in a closed chamber over about 1 week. The evaporation of chloroform was slowed by placing a 20-mL vial containing 5 mL chloroform inside the chamber. The resulting samples were placed under vacuum at room temperature overnight to remove any residual solvent.

2.5 Heat Treatment

The carbonyl ligands on the dicobalt hexacarbonyl metal complex were removed upon a heat treatment using a Barnstead Thermolyne 79,300 single zone tube furnace. Under vacuum, the solvent-annealed sample was first heated to 110 °C for 10 min at a rate of 10 °C/min, and then heated to 200 °C for 360 min at the same rate. The

sample was then allowed to cool down to room temperature. The color of the sample turned from red to black after the heat treatment, indicating the decomposition of the metal complex.

2.6 Morphology Characterization

The bulk morphologies of the samples both before and after the heat treatment were characterized by transmission electron microscopy (TEM) and small-angle X-ray scattering (SAXS). First, sections with a 40–50 nm thickness were obtained by cryo-microtoming the bulk samples using a Leica Ultracut UCT microtome equipped with a Leica EM FCS cryogenic sample chamber operated at −110 °C, and collected on TEM grids. These unstained sections were then imaged using a JEOL 100CX TEM operating at an accelerating voltage of 100 kV. Samples for SAXS were prepared by sandwiching the bulk samples in between two Kapton® films. SAXS patterns were obtained from an Osmic MaxFlux Cu Kα X-ray source with a wavelength of 1.54 Å (Molecular Metrology, Inc.) and a two-dimensional gas-filled wire array detector (Molecular Metrology, Inc.) at a distance of 1,476 mm from the sample. The raw data were calibrated for the peak position with the silver behenate standard, which has a peak position at scattering vector $q = 1.076\ \mathrm{nm}^{-1}$. Two-dimensional images were reduced to the one-dimensional form using angular integration. Scattering vectors (q) were calculated from the scattering angles (θ) using $q = 4\pi \sin\theta/\lambda$, and d-spacings were calculated from the principal scattering maxima (q^*) using $d = 2\pi/q^*$.

2.7 Magnetic Property Characterization

The bulk samples, after heat treatment, were ground into powders in liquid nitrogen and filled into a gelatin capsule, which were then inserted into a straw and carefully transferred to an appropriate holder in a Quantum Design Magnetic Property Measurement System (MPMS®). The magnetic hysteresis curves at room temperature were recorded on the SQUID by varying the magnetic field from −10,000 to +10,000 oersteds (Oe). Magnetic parameters, including coercivity (H_c), saturation magnetization (M_s) and remnant magnetization (M_r), were determined from these magnetic hysteresis curves.

3 Results and Discussion

3.1 Synthesis

The *exo*-oxanorbornene backbone was used for both the alkyl- and cobalt-containing monomers to provide easy functionalization and excellent initiation between blocks (Fig. 1). The alkyl chain length of monomer **2** influences the microphase separation of the resulting BCPs, and a length of 16 (C_{16}) was chosen based on previous studies in which it exhibited the most well-defined microdomains [17]. BCPs with a C_{16} block and a Co block were synthesized by sequentially adding monomers **2** and **4** to the third generation Grubbs' catalyst (G3), as shown in Fig. 1. G3 has proven to be compatible with the dicobalt hexacarbonyl metal complex, and the living polymerization of monomer **4** has been demonstrated [18], which is essential to produce the well-defined diblock architecture. The synthesis of each block required no more than 15 min, and the monomer conversions for all of the polymers were above 95 %.

To study the effect of domain size on the magnetic properties of the nanostructured BCP materials, a series of five BCPs with various molecular weights and constant block ratios were synthesized. All the BCPs exhibited a monomodal and narrow molecular weight distribution, as shown in Fig. 2. As molecular weight increased from **Poly1** to **Poly5**, the primary peak of the GPC curves shifted to lower retention time. Narrow minor peaks (<3 % of

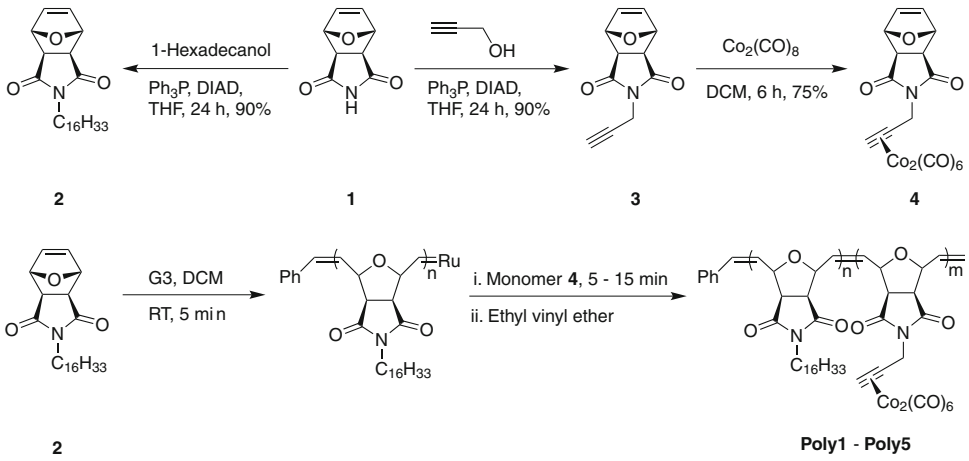

Fig. 1 Synthesis of monomers, **2–4**, and cobalt-containing diblock copolymers with various molecular weights and constant block ratios, **Poly1–Poly5**

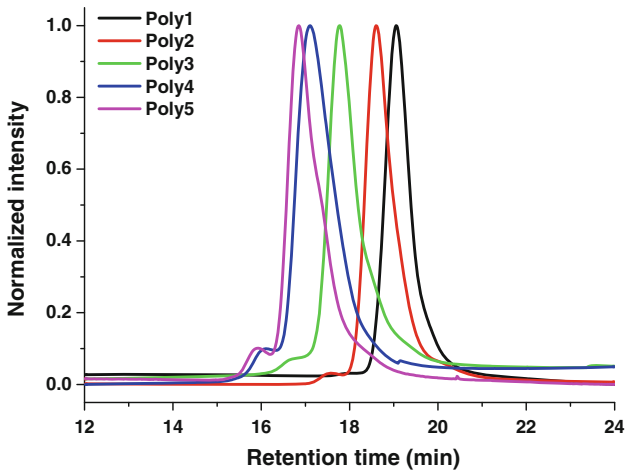

Fig. 2 Representative GPC curves for the cobalt-containing diblock copolymers with various molecular weights, **Poly1–Poly5**

total) at about twice the molecular weight of the primary peaks were occasionally observed and became more obvious for higher molecular weight BCPs. These high molecular weight bumps in GPC curves were previously reported in the literature [21], and were likely attributed to acyclic/secondary metathesis competing with ROMP [22, 23]. Since higher molecular weight BCPs needed longer polymerization time, the chances for acyclic/secondary metathesis increased as well, leading to more noticeable higher molecular weight components in the GPC curves.

3.2 Self-Assembly of the Cobalt-Containing Diblock Copolymers

The molar ratios of the C_{16} units to the Co units in all the BCPs were held constant (70:30) to ensure the same phase-separated morphology, as the morphology influences the magnetic properties of nanostructured BCP materials [17]. Solvent annealing was utilized to induce the self-assembly of the cobalt-containing diblock copolymers. SAXS and transmission electron microscopy (TEM) were used to characterize the morphologies of the resulting samples. After solvent annealing, the SAXS profiles of the BCPs all showed peaks corresponding to q^*, $\sqrt{3}q^*$, and $\sqrt{7}q^*$ (q^* denotes the primary scattering peak), indicating cylindrical morphologies. A representative SAXS profile for **Poly4** is shown in Fig. 3a. Figure. 3b shows a representative bright field TEM image of the unstained, solvent-annealed sample, further confirming the formation of well-defined, phase-separated nanodomains. The dark contrast of the cylindrical domains is attributed to the presence of the heavy cobalt atoms.

The compositional details of all five BCPs are listed in Table 1. As the molecular weight of the BCPs increased from 52 to 296 kDa, the *d*-spacing increased from 32 to 52 nm (1.6 times), which was calculated from the SAXS data according to the equation $d = 2\pi/q^*$. Meanwhile, the diameter of the cobalt-containing cylindrical domains, which was obtained from the TEM images, increased 1.6 times as well, from 16 to 25 nm. The nanostructured BCPs were then converted to RTFMs upon a simple heat treatment according to established procedures [17]. It has also been demonstrated in our previous studies that the phase-separated morphology was intact after the heat treatment.

3.3 Magnetic Properties of the Nanostructured Diblock Copolymers After Heat Treatment

The magnetization as a function of the applied field (*M–H*) was measured at room temperature by SQUID for all of the nanostructured BCP materials after heat treatment. Magnetic hysteresis loops were observed for all the samples (Fig. 4), indicating that they were all RTFMs.

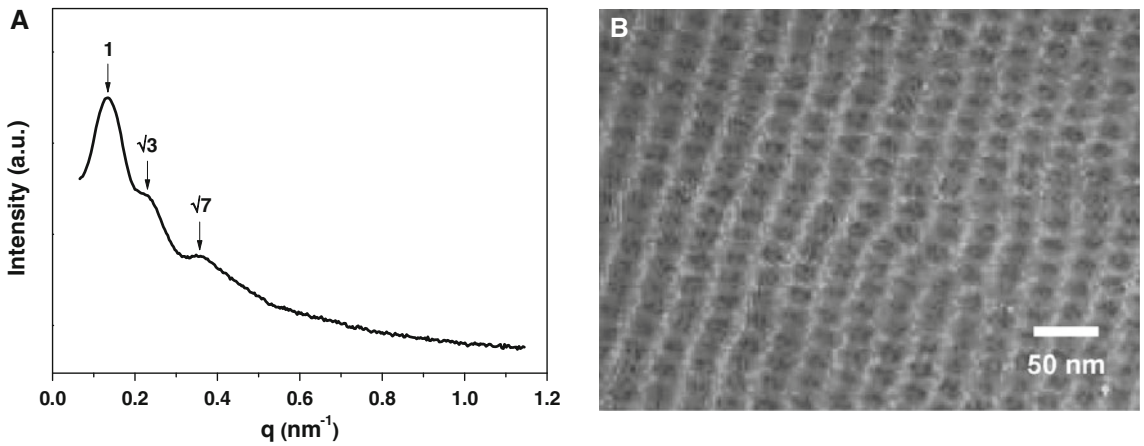

Fig. 3 Representative **a** SAXS curve and **b** TEM micrograph of a cobalt-containing diblock copolymer (**Poly4**) after solvent annealing in chloroform

Table 1 Characterization of the cobalt-containing diblock copolymers

Polymer	M_n (kDa)[a]	M_w (kDa)[a]	PDI[a]	Morphology	d-Spacing (nm)[b]	d_{cyl} (nm)[c]
Poly1	52	58	1.11	Cylindrical	32	16
Poly2	100	112	1.12	Cylindrical	38	20
Poly3	196	216	1.10	Cylindrical	43	22
Poly4	262	318	1.21	Cylindrical	48	24
Poly5	296	370	1.25	Cylindrical	52	25

Poly1–Poly5, with various molecular weights and constant block ratios

[a] Determined by GPC in THF using RI detector, relative to polystyrene standards

[b] Bulk periodicity: $d = 2\pi/q^*$, where q^* is the primary scattering peak as determined by SAXS

[c] The diameter of the cylindrical domains (d_{cyl}) was determined from the TEM images

The coercivity values at room temperature (in Oe) were obtained from the x-intercepts of the hysteresis loops and are plotted as a function of the cylindrical domain size, as shown in Fig. 5. The difference in coercivity values for these nanostructured BCP materials with various cylindrical domain sizes was statistically not significant, as the error bars overlapped with each other. Previously, it was determined that the superparamagnetic to ferromagnetic transition of cobalt nanoparticles occurs around 10–12 nm in size at room temperature [24]. Given that the cylindrical domain size investigated here was varied from 16 to 25 nm, the critical dimensions may not have been explored. According to theoretical calculation, the domain size (or d-spacing) of phase-separated diblock copolymers is proportional to $\chi N^{1/6}$ (χ is Flory–Huggins interaction parameter, N is degree of polymerization) [25]. Since χ is constant at a given temperature and polymer composition [26, 27], both the logarithms of d-spacing and cylindrical domain size increased almost linearly with the logarithm of molecular weight of our BCPs (Fig. S1). The slopes are close to the theoretical predicts. As a result, the theoretical domain size of the BCP with molecular weight of 25 kDa can be estimated to be around 14 nm. However, the 25 kDa BCP did not give well-defined phase-separated nanodomains, suggesting that it was not possible to obtain BCPs with a cylindrical domain size smaller than 15 nm for our system. Meanwhile, the BCP with a molecular weight beyond 300 kDa was also difficult to obtain, because the acyclic/secondary metathesis competing with ROMP became more significant with increasing molecular weight and the first block could not be completely initiated by the second monomer to give a monomodal diblock polymer GPC curve. Alternatively, it is possible that the cylindrical domain size does not play a critical role in influencing the magnetic properties of our nanostructured BCP materials, as the cobalt density in the domains is constant.

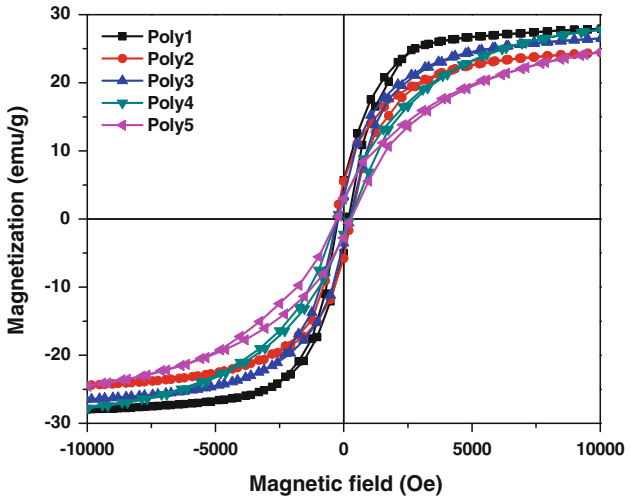

Fig. 4 Magnetization curves of the cobalt-containing diblock copolymers with various molecular weights and constant block ratios, **Poly1–Poly5**

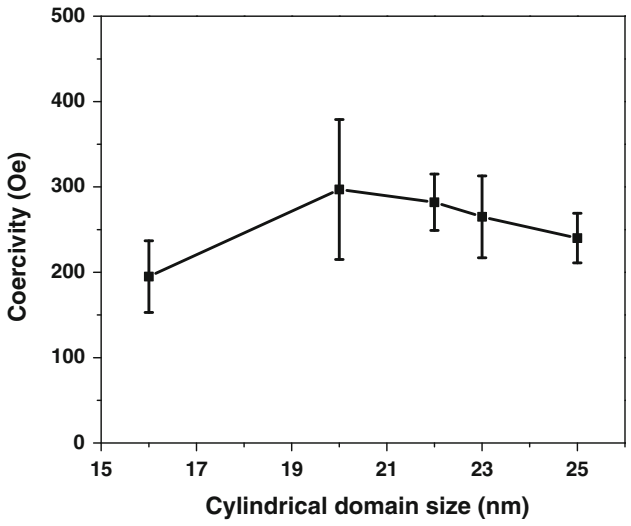

Fig. 5 Influence of domain size on the coercivity of the cobalt-containing diblock copolymers with cylindrical morphologies (standard errors were calculated from three samples)

4 Conclusions

Cobalt-containing diblock copolymers with various molecular weights and constant block ratios were synthesized by ROMP and generated cylindrical morphologies with different domain sizes after solvent annealing. The nanostructured diblock copolymers were all converted to RTFMs upon a simple heat treatment. The coercivity of the nanostructured BCP materials did not show a strong dependence on the domain sizes. This result could be due to the relatively narrow domain size range investigated or a negligible change in cobalt–cobalt dipolar interactions following the change of domain sizes. Compared to our previous studies, domain size seems to play a less important role in determining the magnetic properties of nanostructured BCP materials than morphology and cobalt density. However, the consistent room temperature ferromagnetic properties demonstrate the robust qualities of these cobalt-containing BCP materials.

Acknowledgments We acknowledge the support of Army Research Office (Grant W911NF-09-1-0373) for funding this work. We are also grateful for the support of the Materials Research Science and Engineering Center (MRSEC) at the University of Massachusetts Amherst (DMR-0820506). The authors would like to thank Ms. Catherine N. Walker and Ms. Katherine A. Gibney for assisting manuscript preparation.

References

1. D.L. Leslie-Pelecky, R.D. Rieke, Chem. Mater. **8**, 1770 (1996)
2. C.B. Murray, S.H. Sun, H. Doyle, T. Betley, MRS Bull. **26**, 985 (2001)
3. Y.W. Jun, J.W. Seo, J.W. Cheon, Acc. Chem. Res. **41**, 179 (2008)
4. A. Mehrani, A. Morsali, J. Inorg. Organomet. Polym. **21**, 476 (2011)
5. S.A. Wolf, D.D. Awschalom, R.A. Buhrman, J.M. Daughton, S. von Molnár, M.L. Roukes, A.Y. Chtchelkanova, D.M. Treger, Science **294**, 1488 (2001)
6. N.V. Myung, D.Y. Park, B.Y. Yoo, P.T.A. Sumodjo, J. Magn. Magn. Mater. **265**, 189 (2003)
7. N.A. Kotov, J.O. Winter, I.P. Clements, E. Jan, B.P. Timko, S. Campidelli, S. Pathak, A. Mazzatenta, C.M. Lieber, M. Prato, R.V. Bellamkonda, G.A. Silva, N.W.S. Kam, F. Patolsky, L. Ballerini, Adv. Mater. **21**, 3970 (2009)
8. J.J. Zhao, Z.B. Huang, J.W. Zeng, M. Deng, G.F. Yin, X.M. Liao, J.W. Gu, J. Inorg. Organomet. Polym. **22**, 492 (2012)
9. G.M. Wallraff, W.D. Hinsberg, Chem. Rev. **99**, 1801 (1999)
10. R.B. Grubbs, J. Polym. Sci., Part A: Polym. Chem. **43**, 4323 (2005)
11. I. Dragutan, V. Dragutan, H. Fischer, J. Inorg. Organomet. Polym. **18**, 311 (2008)
12. K.A. Aamer, W.H. De Jeu, G.N. Tew, Macromolecules **41**, 2022 (2008)
13. G.R. Whittell, M.D. Hager, U.S. Schubert, I. Manners, Nat. Mater. **10**, 176 (2011)
14. T. Thurn-Albrecht, J. Schotter, G.A. Kästle, N. Emley, T. Shibauchi, L. Krusin-Elbaum, K. Guarini, C.T. Black, M.T. Tuominen, T.P. Russell, Science **290**, 2126 (2000)
15. J.P. Spatz, S. Mössmer, C. Hartmann, M. Möller, T. Herzog, M. Krieger, H.G. Boyen, P. Ziemann, B. Kabius, Langmuir **16**, 407 (2000)
16. D.A. Rider, K. Liu, J.C. Eloi, L. Vanderark, L. Yang, J.Y. Wang, D. Grozea, Z.H. Lu, T.P. Russell, I. Manners, ACS Nano **2**, 263 (2008)
17. Z.M. Al-Badri, R.R. Maddikeri, Y. Zha, H.D. Thaker, P. Dobriyal, R. Shunmugam, T.P. Russell, G.N. Tew, Nat. Commun. **2**, 482 (2011)
18. Z.M. Al-Badri, G.N. Tew, Macromolecules **41**, 4173 (2008)
19. J.A. Love, J.P. Morgan, T.M. Trnka, R.H. Grubbs, Angew. Chem. Int. Ed. **41**, 4035 (2002)
20. H. Kwart, I. Burchuk, J. Am. Chem. Soc. **74**, 3094 (1952)
21. S.T. Trzaska, L.B.W. Lee, R.A. Register, Macromolecules **33**, 9215 (2000)
22. L.B.W. Lee, R.A. Register, Polymer **45**, 6479 (2004)
23. R. Walker, R.M. Conrad, R.H. Grubbs, Macromolecules **42**, 599 (2009)
24. J.I. Park, N.J. Kang, Y.W. Jun, S.J. Oh, H.C. Ri, J. Cheon, ChemPhysChem **3**, 543 (2002)
25. G.M. Grason, Phys. Rep. **433**, 1 (2006)
26. F.S. Bates, Science **251**, 898 (1991)
27. A.J. Nedoma, M.L. Robertson, N.S. Wanakule, N.P. Balsara, Ind. Eng. Chem. Res. **47**, 3551 (2008)